

Article

On the Quality of Protein Crystals Grown under Diffusion Mass-transport Controlled Regime (I)

José A. Gavira ¹, Fermín Otálora ¹, Luis A. González-Ramírez ¹, Emilio Melero ¹,
Alexander E.S. van Driessche ² and Juan Manuel García-Ruíz ^{1,*}

¹ Laboratorio de Estudios Cristalográficos, Instituto Andaluz de Ciencias de la Tierra (Consejo Superior de Investigaciones Científicas-Universidad de Granada), Avenida de las Palmeras 4, 18100 Armilla, Granada, Spain; jgavira@iact.ugr-csic.es (J.A.G.); fermin@lec.csic.es (F.O.); luis.gonzalez@csic.es (L.A.G.-R.); emilio.melero.garcia@gmail.com (E.M.)

² Université Grenoble Alpes, Université Savoie Mont Blanc, CNRS, IRD, IFSTTAR, ISTerre, F-38000 Grenoble, France; alexander.van-driessche@univ-grenoble-alpes.fr

* Correspondence: juanma.garcia.ruiz@gmail.com

Received: 24 December 2019; Accepted: 22 January 2020; Published: 25 January 2020



Abstract: It has been previously shown that the diffraction quality of protein crystals strongly depends on mass transport during their growth. In fact, several studies support the idea that the higher the contribution of the diffusion during mass transport, the better the diffraction quality of the crystals. In this work, we have compared the crystal quality of two model (thaumatin and insulin) and two target (HBII and HBII-III) proteins grown by two different methods to reduce/eliminate convective mass transport: crystal growth in agarose gels and crystal growth in solution under microgravity. In both cases, we used identical counterdiffusion crystallization setups and the same data collection protocols. Additionally, critical parameters such as reactor geometry, stock batches of proteins and other chemicals, temperature, and duration of the experiments were carefully monitored. The diffraction datasets have been analyzed using a principal component analysis (PCA) to determine possible trends in quality indicators. The relevant indicators show that, for the purpose of structural crystallography, there are no obvious differences between crystals grown under reduced convective flow in space and convection-free conditions in agarose gel, indicating that the key factor contributing to crystal quality is the reduced convection environment and not how this reduced convection is achieved. This means that the possible detrimental effect on crystal quality due to the incorporation of gel fibers into the protein crystals is insignificant compared to the positive impact of an optimal convection-free environment provided by gels. Moreover, our results confirm that the counterdiffusion technique optimizes protein crystal quality and validates both environments in order to deliver high quality protein crystals, although other considerations, such as protein/gel interactions, must be considered when defining the optimal crystallization setup.

Keywords: protein crystallization; microgravity; agarose; counterdiffusion

1. Introduction

Obtaining crystals of sufficient quality is essential for obtaining good diffraction data and building accurate 3D structural models of both small and macromolecules. It is widely accepted that this is the main bottleneck in structural biology studies, which results in slowing down the drug design process. Many strategies, recalled in this Special Issue, have been assayed not only to obtain initial 3D models from X-ray data but also to improve crystal quality, a fundamental requirement in drug design. Consequently, it is not surprising that crystallization in space has received much financial support from both public space agencies and private companies until the last decade [1]. Since the early

protein crystallization space adventure in 1984, many instruments have been tested under microgravity conditions [2–7]. At first, the results were not very conclusive, but interest did not decline, leading to a vast amount of research into reduced gravity environments [2–7], most of which reported crystal quality enhancements and strongly contributed to a better understanding of the nucleation and growth of protein crystals [4,8–10]. Although several parameters, such as the isoelectric point and water content, were not considered when analyzing the results, the observed improvement in crystal quality was explained on the basis of reduced crystal sedimentation, density-driven convection flows provoking the formation of depletion zones around growing crystals [11–14], and the reduced incorporation of impurities [4,15,16]. The formation of a stable depletion zone in diffusive setups minimizes and stabilizes the supersaturation at the crystal/solution interface, reducing and making constant the growth rate, which kinetically favors the arrangement of molecules at the crystal surface and allows for efficient transport of impurities out of it. This is generally accepted as a factor enabling crystal perfection [17–20]. Therefore, it was concluded that the diffusive mass-transport conditions created during microgravity experiments are a key factor in obtaining good quality protein crystals [21,22].

This agreed beneficial effect of the diffusive mass-transport regime on crystal quality, together with the economic costs associated with experiments in space, were the driving force when considering further existing ground-based alternatives to mimic this specific mass-transport scenario [23]. Several approaches have been proposed to eliminate/reduce gravity-induced convection on Earth [24–30], but one of the most commonly used techniques, due to its ease of implementation, is that of gelling the growth media [31–33]. Agarose, a thermo-reversible hydrophilic hydrogel, is the most commonly used gelling additive due to its frequent use in bio-laboratories and its ease of preparation. Agarose gels behave as a neutral network in which convection is reduced or eliminated (depending on concentration [34]) and supersaturation at the crystal surface is homogeneous and steady [35]. In addition, sedimentation is avoided, favoring three dimensional growth, and impurity incorporation is reduced [36,37], leading to better-diffracting crystals [31,38], even though gel fibers are incorporated within the protein crystal lattice independently of gel and protein nature [39–42]. However, an exhaustive rational comparison between crystals grown in a mass diffusive growth media created by microgravity and those grown in gel media on-ground should be carried out in order to validate this alternative to microgravity diffusive environments. Only on rare occasions have crystals grown under microgravity in solution been compared with gel-grown protein crystals from underground gravity conditions [43–45], and only once at two levels of gravity [38]. Among these works, only Evrard and co-workers [44] have presented a systematic study on the crystallization of TIM (triosephosphate isomerase) from solution in microgravity and gel on-ground, concluding that under low gravity conditions crystals were slightly better. However, their experiments did not allow them to pinpoint the reason behind this observation.

We have conclusively shown that counterdiffusion methods produce crystals of higher quality than conventional convective crystals (hanging/sitting, drop, batch, etc.) [27], but after more than 25 years of investigation, there is still no clear picture of the possible advantages of microgravity conditions over on-ground gel growth in terms of protein crystal quality [4,7,46,47]. This can, in part, be due to the difficulty of controlling microgravity conditions with precision (i.e., G-jitters, residual acceleration, lack of consistent data on microgravity levels during experiments, etc.) or the poor control of temperature during microgravity experiments. Additionally, sample handling during pre- and post-flight operations (temperature, vibration, aging, etc.) before X-ray data collection can have a large impact on data quality and often varies greatly between experiments.

This work addresses the missing comparison in terms of crystal quality between diffusive crystal growth setups, both on-ground and in microgravity. We have compared several X-ray quality indicators for protein crystals (model and target) grown using identical experimental conditions (e.g., protein and reactant batches, crystallization hardware, thermal history, handling, storage, and transportation) in two different reduced convection environments: microgravity and gels. The microgravity experiments were run in a small unmanned spacecraft (Foton M3) to ensure the best possible microgravity scenario

(very small g-level). Ground experiments were set up at the same time, using the same reactors, chemicals, and procedures. A specific protocol was defined for synchrotron radiation data collection and analysis to evaluate crystal quality.

2. Materials and Methods

2.1. Crystallization Experiments

For the experiments we selected two model proteins, bovine pancreas insulin and thaumatin from *T. daniellii*, purchased as lyophilized powder from Sigma (I5500 and T7638 respectively), and two target systems, hemoglobins HBII and HBII-III from *L. pectinata* [45] kindly provided by the group of Prof. Juan Lopez-Garriga from the University of Puerto Rico at Mayagüez. Thaumatin and insulin were dissolved in MilliQ water. Protein concentration was determined spectrophotometrically at 280 nm prior to setting up the crystallization experiments and after filtration through a 0.45 µm membrane. All other chemicals were of analytical grade and used without further purification.

Experiments were set up to suit the second version of the Granada Crystallization Facility (GCF-2) using two types of reactors, the Granada Crystallization Box-Domino (GCB-D) and the three layer capillaries (3LC), described elsewhere [3]. In short, both the GCB-D and the 3LC reactors exploit the counterdiffusion technique using a middle layer of gel to control the starting time of the experiments, which eliminates the need for any activation. One of the main features of the new GCF is the active control of the temperature ensuring a set point of 20 ± 0.5 °C, not only during the mission but also during transportation. In short, we followed the already described standard procedure in setting up the experiment; i.e., the agarose layer (1.0% *w/v*) was added to the GCB and allowed to set and capillaries, loaded with the protein solution and sealed at the top, were punctuated into the gel layer. For equivalent ground experiments, protein solution was mixed with agarose (0.5% *w/v*) prior to loading the capillaries. The precipitant was then added on top and the GCB sealed. In the case of the 3LC experiment, the protein solution was loaded first (with 0.1% agarose for the ground experiments) and the bottom end of the capillary sealed with beeswax. Then, the second layer of agarose was added with the help of a Pasteur pipette and allowed to set. Finally, the precipitant solution was poured on top of the agarose layer and the system sealed with beeswax. Two identical units of the GCF-2 were prepared on site for the space and ground experiments. The experimental conditions are summarized in Table 1.

Table 1. Summary of the crystallization conditions. For ground experiments 0.1%–0.3% (*w/v*) agarose was added to the protein chamber.

Protein	Concentration (mg/mL)	Precipitating Agent	Buffer	Type
Thaumatin	50	2.4 M NaK-tartrate	0.1 M Hepes pH 7.0	GCB
Insulin	30	25% PEG 4000, 0.2 M NaK-tartrate	0.02 M Na Phosphate pH 10.5, 0.02 M EDTA	3L
HBII-O2	30	5 M Na Formate pH 5.0	Water	3L
HBII-III-CN	30	5 M Na Formate pH 5.0	Water	3L

2.2. X-ray Data Collection and Analysis

Crystal quality was determined from X-ray diffraction data collected at beam line BM16 of the European synchrotron radiation facility (ESRF). Crystals were extracted from the hydrogel or the capillary using a cut pipette tip and deposited on a plastic Petri dish. Drops of the recovered precipitant or the precipitant plus cryoprotectant (20% *v/v* glycerol) were deposited nearby. Selected crystals were transferred to the cryoprotectant solution and equilibrated for 10 to 20 seconds before being mounted manually in the goniometer-head and flash-cooled. The data collection protocol was the same for all crystals as summarized in Table 2. We collected a total of 42 full datasets, 23 in space and

19 on-ground. All datasets were integrated, scaled, and merged using Denzo and Scalepack [48] and the main indicators extracted from the final log files (data are compiled in Tables S1–S4).

Table 2. X-ray data collection protocol.

Protein	Dose Mode	Rotation	Detector-Crystal	N° Frames	Temperature
HBII-O2	Fixed	0.5°	183 mm	300	100 K
HBII-III-CN	Fixed	0.5°	196 mm	275	100 K
Insulin	Fixed	0.5°	124 mm	150	100 K
Thaumatococcus	Fixed	0.5°	120 mm	180	100 K

2.3. Principal Component Analysis

A comprehensive set of data quality indicators, derived from the data reduction and merging steps, was selected for statistical quality analysis. These ten indicators, tabulated in Table S1, include the completeness of the full dataset and the highest resolution shell (Comp, CompH); redundancy (Redund, RedundH); R_merge (Rmerge, RmergeH); intensity over noise (IoSigma, IoSigmaH); B-factor (Bfactor); and mosaic spread (Mosaic). Table S5 also lists the crystal code, the corresponding protein (hb2 = oxy-hemoglobin II, hb23 = cyano-hemoglobin II-III, ins = insulin, th = thaumatococcus) and a flag indicating if the crystal was grown in space or ground conditions (s = space and g = ground).

Comparison of the quality indicators, because of an inherently different space group, resolution limit, etc., is not possible without a normalization of the distribution of indicator values. To obtain a zero-centered distribution, the mean of the distribution was first subtracted from each value and then all values were divided by their standard deviation. This scaling was done for each protein separately using both space and ground indicators to compute the mean and standard deviation. In this way, differences in crystal quality between space and ground crystals can be identified by differences in the indicator distribution while distributions for different proteins are still comparable. Table S2 shows the normalized data for all crystals used in this study.

3. Results

Among the many relevant parameters to be considered when comparing crystal quality, two are of paramount importance: microgravity level and temperature, along with the stability of those parameters during the growth process. The Granada Crystallization Facility (GCF-2) and the supporting ground electronics device (GSE) keep the temperature of the reactors at 20 °C with an accuracy of ± 0.5 °C. Accelerometric data provided by other instruments onboard Foton M3 were also tracked, showing a very low overall g-level, which increased steadily from 0.5 to 5.5 μG (Figure 1). During the whole mission, the gravity level was always below 8 μG . According to Carotenuto and co-workers [49], at this level of residual gravity buoyancy-driven convection of the fluid can be completely neglected. These data also suggested that low frequency vibrations, correlated in previous studies with the movement of the crystals and the variation of their growth rate [46], were below 10 $\mu\text{g}^2/\text{Hz}$ in the 1–10 Hz range during the whole mission, small enough to be negligible.

Visual inspection of the experiments after landing showed that both the space-grown crystals and their on-ground counterparts contain good-looking crystals with no significant differences in terms of nucleation density, crystal size, or surface defects. Figure 2 shows representative crystals of insulin (model protein) and oxy-hemoglobin II, II-III (target protein) grown both in space and on-ground.

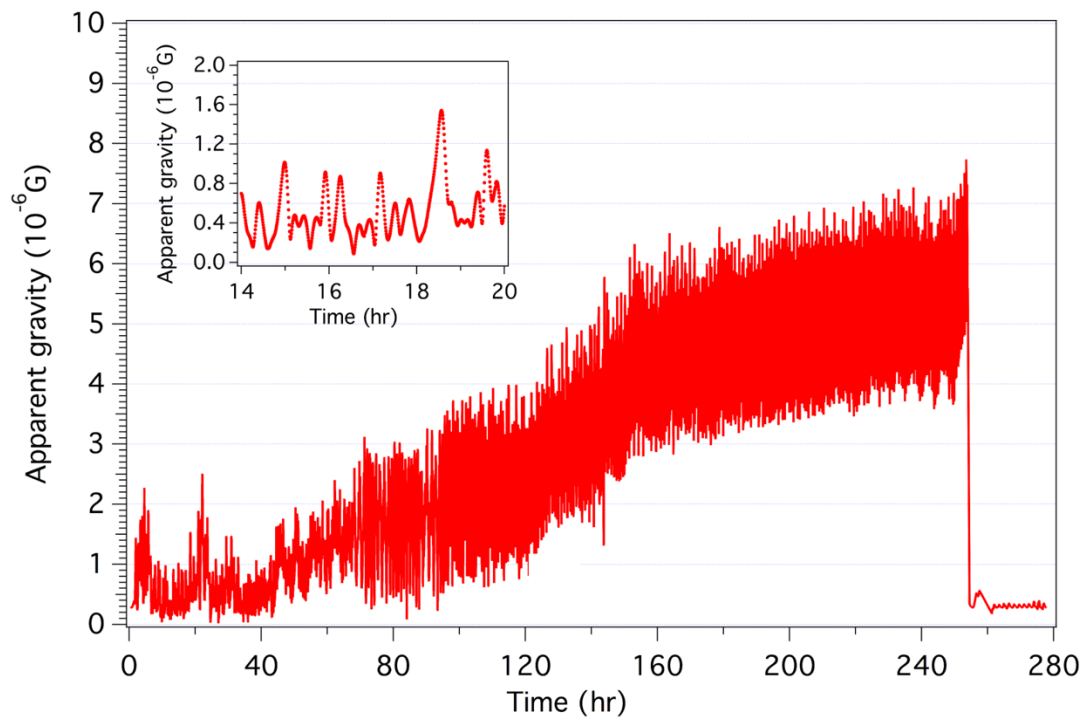


Figure 1. Modulus of the apparent gravity (residual acceleration) as a function of the time (0 is the beginning of the mission). The insert corresponds to the first six hour interval showing the amplitude and duration of the standard oscillation of the gravity level.

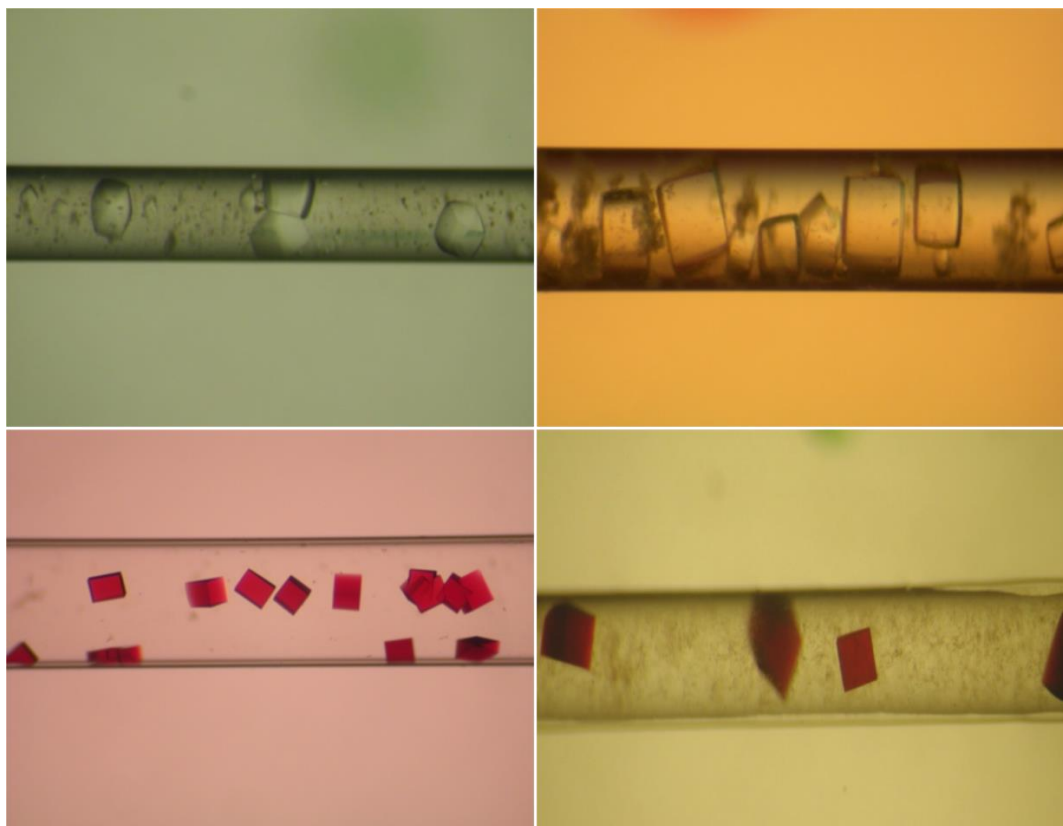


Figure 2. Pictures showing crystals of insulin (top, $\Phi_{\text{inner}} = 0.5$ mm) and cyano-HbII-III (bottom, $\Phi_{\text{inner}} = 0.7$ mm) proteins grown in space (left) and on-ground in agarose gel (right) environments, respectively.

For structural biology studies, the best protein crystals are those producing the better diffraction data, in order to accurately determine the 3D structural model of the target protein [6,18]. As a rule of thumb, the quality of a crystal depends on two key factors: the coherent attachment of the molecules to the crystal lattice and the amount of impurity incorporated in the crystal volume, which can produce lattice strain [50]. The first factor is directly related to the supersaturation and supersaturation rate, and a correlation has been found between low supersaturation and better lattice order [51]. Not only does supersaturation matter, but the steadiness of the supply of molecules during growth also plays a role in avoiding the formation of zonal defects, such as striations, by maintaining a constant supply of molecules and a constant impurity ratio. This scenario is broken by convective mass transport that distorts and/or destroys the depletion zone around growing crystals [6,18]. In this study, we will compare crystals grown in two scenarios with minimized convection.

The normalized data shown in Table S6 were used to compare space and ground crystals for each of the ten selected quality indicators. The Tukey [52] five number summaries (minimum, lower-hinge, median, upper-hinge, maximum) calculated for each indicator are presented in Figure 3 and listed in Table S7. From this analysis, we can observe that the data collected from crystals grown in space is better in terms of overall completeness, redundancy at high resolution, and mosaic spread, but is almost equal to the ground crystal indicators in terms of completeness at high resolution, overall redundancy, and B factor. On the other hand, crystals grown on-ground are better in terms of Rmerge and signal over noise ratio, but in all cases the differences are small, always equal to or lower than 0.5 times the standard deviation. A comparison of the distribution shows that the differences in all indicators are not statistically significant with p-values higher than 30% for all indicators except for the mosaic spread (15.7%) indicating larger, but still not significant, differences. The standard deviation of most of the indicators is smaller for the space-grown crystals than for on-ground. This observation could be related to a higher homogeneity of the crystal's environment and, therefore, crystal quality.

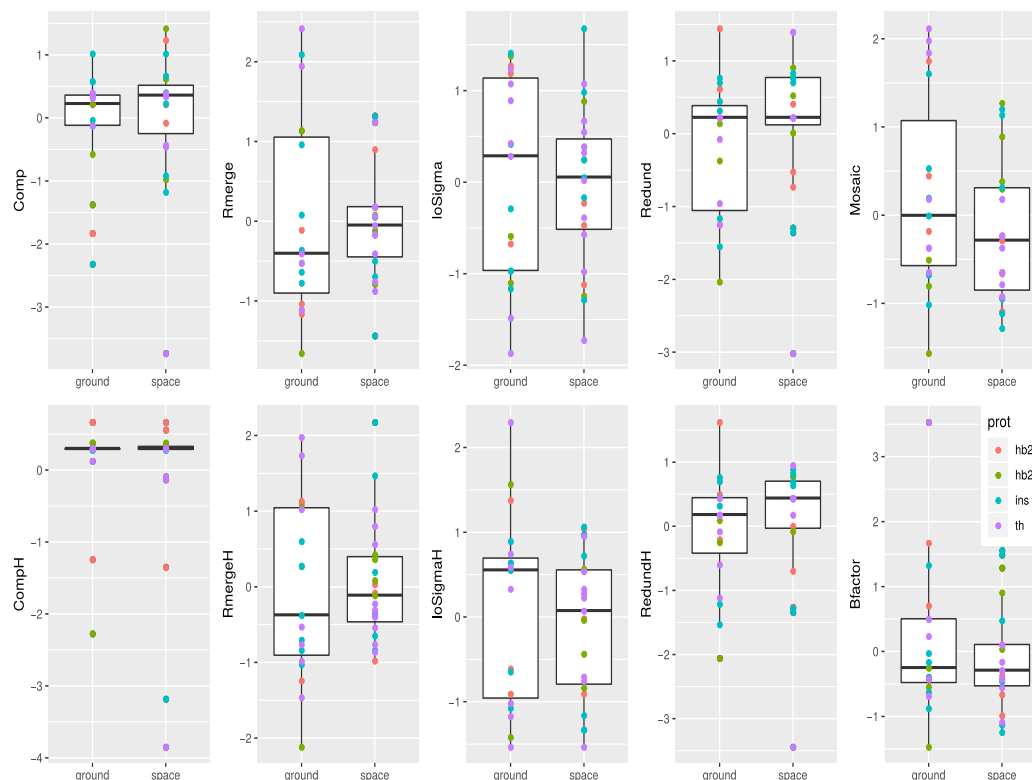


Figure 3. Minimum, lower-hinge, median, upper-hinge, and maximum for each of the ten analyzed indicators is shown as box plots of the values obtained from the two (space/ground) populations. The individual values are over-plotted as circles colored according to the protein.

A similar previously reported analysis of ferritin crystals grown in solution on-ground and under low gravity conditions shows a significant correlation between quality indicators [53]. Therefore, a principal component analysis (PCA) [54,55] was performed to check for any trends in quality indicators that could be hidden in this multidimensional set of indicators. As shown in Figure 4 (Table S8), the PCA analysis highlights the correlation between different indicators, i.e., 58.3% of the variance of the dataset can be explained by just two dimensions and up to 76.3% of the variance is described by adding a third dimension.

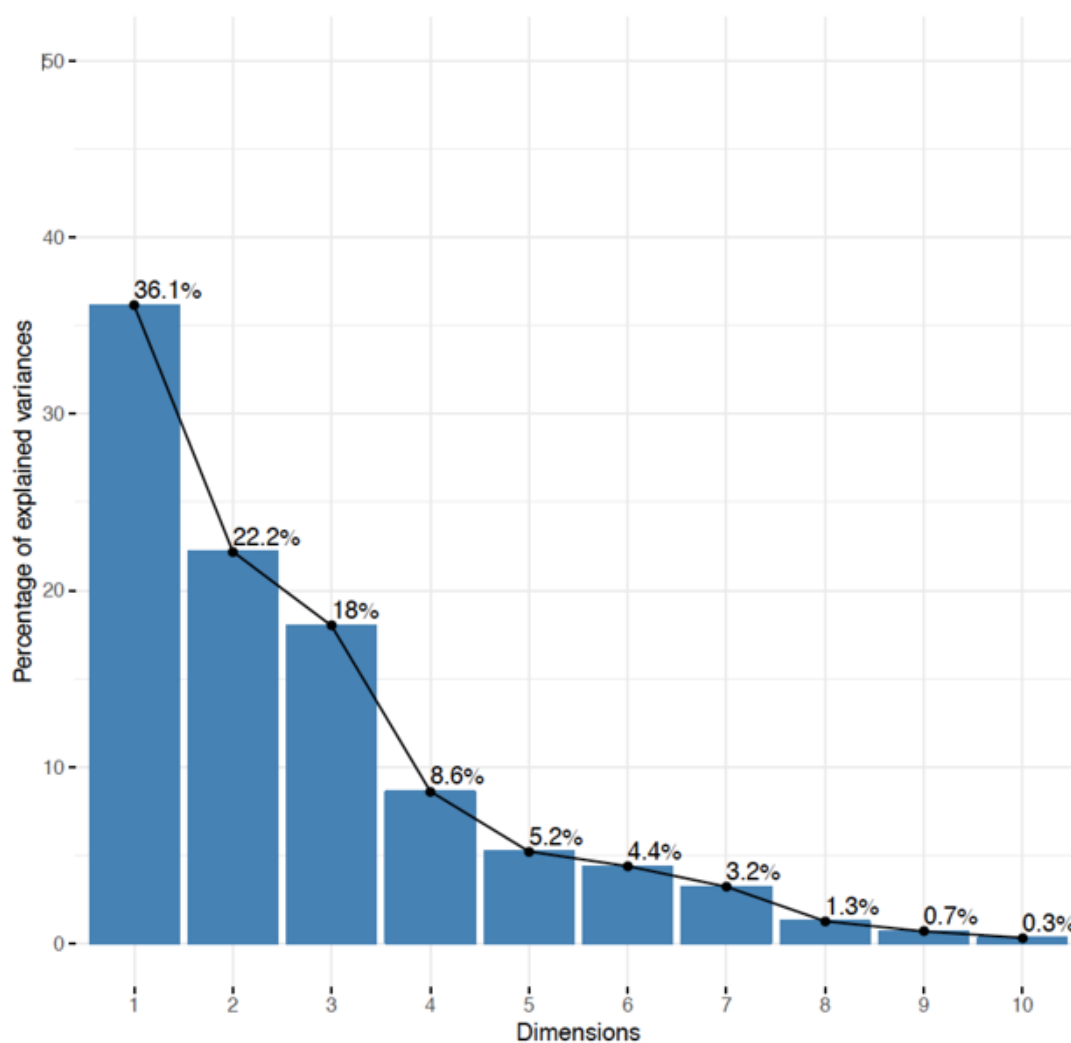


Figure 4. Percentage of variance explained by each of the ten dimensions obtained by PCA analysis of the distributions of quality indicator values.

We can now analyze how much each indicator contributes to each dimension, although for our purpose, it is enough to consider just the fifth dimension, which already explains more than 90% of the variance. Figure 5 (Table S9) shows the contribution of each of the ten indicators analyzed in the direction of the first five dimensions. Dimension 1 is mostly in the direction of redundancy (overall and high resolution) and intensity over noise (mainly overall) with important contributions of completeness and R-merge at high resolution. Dimension 2 is relatively aligned with overall R-merge, completeness, and R-merge at high resolution. B-factor also contributes significantly.

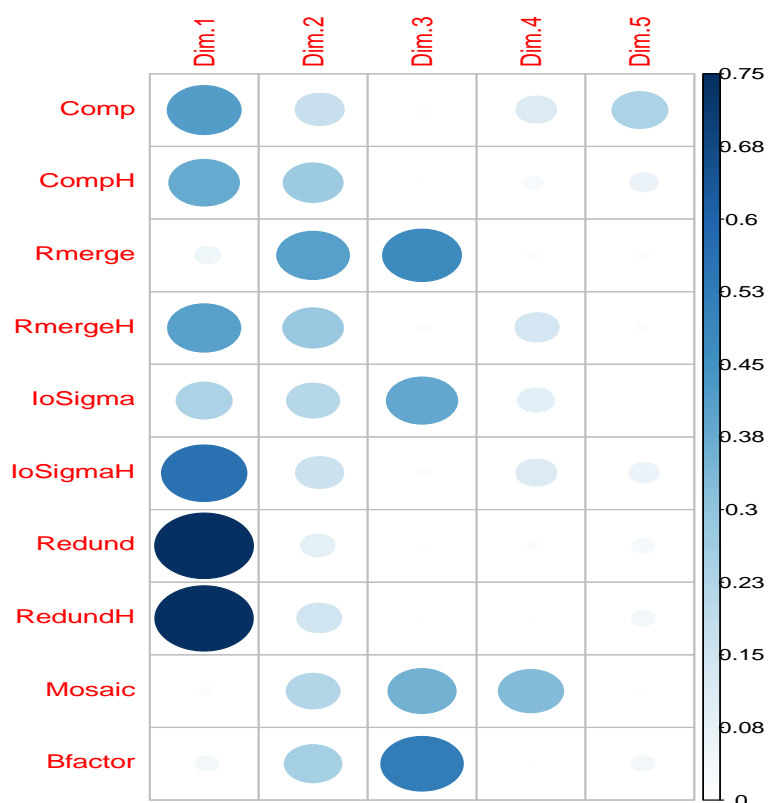


Figure 5. Contribution of each indicator to the five first dimensions.

We can now summarize the results of the principal component analysis of our set of indicators in a single representation. Figure 6 represents the contribution of the ten indicators to the first two dimensions (58.3% of the variance of the datasets). As anticipated, indicators are highly correlated, showing as nearby vectors, with completeness and redundancy (overall and high resolution in both cases) making a set of highly correlated values. R-merge, intensity over noise, B-factor, and mosaic spread fall into a second set of highly correlated indicators (negatively correlated in the case of intensity over noise because the value increases for higher quality, while those of the other correlated indicators decrease). The space-grown crystals showed larger variance along the completeness/redundancy axis while ground crystals were less spread in this direction and showed larger spread along the R-merge, B-factor, mosaic spread and intensity over noise directions. In any case, the differences between the indicators of the two groups are small.

Interestingly Dimension 3 (explaining 18% of the variance) in the PCA analysis is aligned with R-merge, IoSigma, Mosaic, and B-factor (Figure 5), the most typical indicators used to define protein crystal quality [53]. This suggests that this dimension could be relevant in terms of crystal quality difference between space and ground crystals, but the two populations are equally indistinguishable (Figure S1) and do not provide new insights.

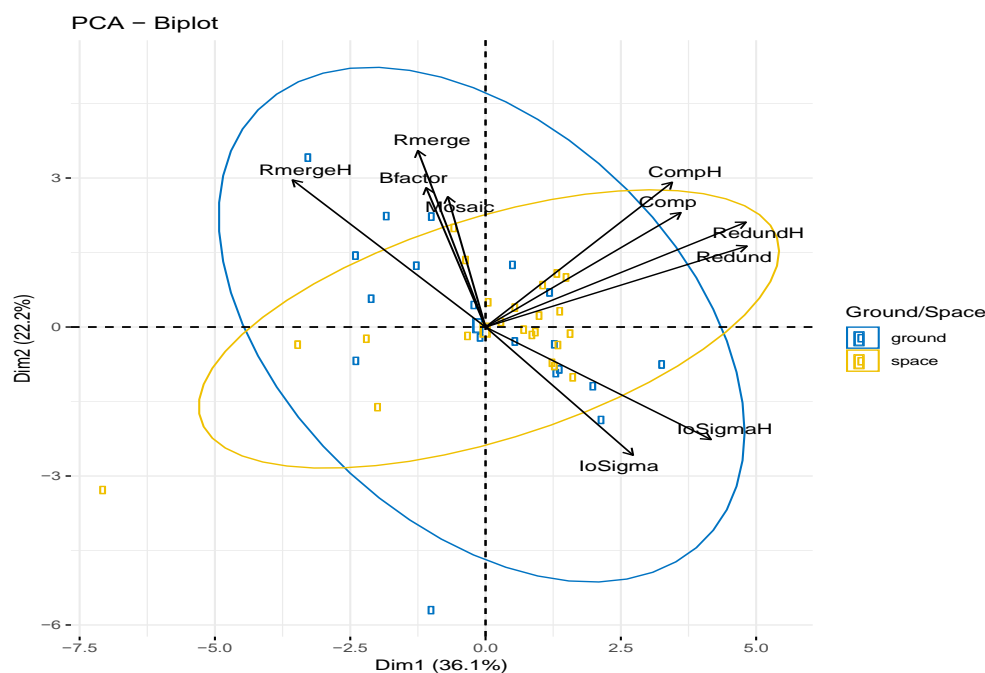


Figure 6. Summary of the PCA analysis on the quality indicators dataset. The plot shows the first and second dimensions of the analysis. The projected direction of each indicator “axis” is indicated by arrows. The indicators for all the crystals in the dataset are plotted as blue/yellow circles for ground/space-grown crystals. The same colors are used to indicate the ellipses encompassing the representative points within the two groups.

4. Conclusions

The role of microgravity in protein crystal quality was investigated by comparing similar—but not identical—mass-transport scenarios dominated by diffusion, i.e., space-grown crystals and crystals grown in gels. Identical counterdiffusion experiments were set up with four proteins keeping constant and careful monitoring of all critical parameters. The crystals characterized in this study have been grown either under perfect diffusive mass-transport conditions in gel media or under reduced convection in space within a crewless rocket, in both cases, at a constant temperature of 20 °C. The high quality of the crystals obtained can be attributed to a) the reduction of convection in the growth environment and b) the experimental counterdiffusion setup that self-searches for the best crystallization conditions within the capillary/reactor.

Our detailed X-ray diffraction analysis demonstrates that a) all grown crystals diffract at high resolution as expected from the counterdiffusion technique; b) in terms of relevance for structural studies, the crystals grown under microgravity are of similar quality to those grown in gels on Earth. This result is particularly relevant since the incorporation of the gel fibers into the crystals is expected to decrease their quality as they reduce diffraction crystal volume and could increase the disorder of the crystal lattice. Our results show that this reduction of crystal quality, expected due to the incorporation of the gel fibers, is counterbalanced by the perfect diffusive environment (zero convection) provided by the porous gel structure.

All in all, our results show that 1) the growth of crystals in gels is an excellent technique for obtaining protein crystals of the highest quality; 2) the scenario offered by space agencies for the growth of high-quality protein crystals can be enhanced; 3) when a chemically clean environment is needed, space crystallization is a suitable alternative for the growth of high-quality protein crystals; and 4) the counterdiffusion technique is particularly well-suited to perform experiments designed to understand precipitation in space.

Supplementary Materials: The following are available online at <http://www.mdpi.com/2073-4352/10/2/68/s1>, Figure S1: The plot shows the first and third dimensions of the PC analysis. The projected direction of each indicator “axis” is indicated by arrows. The indicators for all the crystals in the dataset are plotted as blue/yellow circles for ground/space grown crystals. The same colors are used to indicate the ellipses encompassing the representative points within the two groups; Table S1: Resume of data collection and refinement statistics for oxy-hemoglobin II crystals grown in space and on-ground; Table S2: Resume of data collection and refinement statistics for cyano-hemoglobin II-III crystals grown in space and on-ground; Table S3: Resume of data collection and refinement statistics of insulin crystals grown in space and on-ground; Table S4: Resume of data collection and refinement statistics of thaumatin crystals grown in space and on-ground; Table S5: Quality indicators from dataset processing including the completeness of the full data set and the highest resolution shell (Comp, CompH), redundancy (Redund, RedundH), R_merge (Rmerge, RmergeH), intensity over noise (IoSigma, IoSigmaH), B factor (Bfactor) and mosaic spread (Mosaic). The codes identify the proteins (hb2 = oxy-hemoglobin II, hb23 = cyano-hemoglobin II-III, ins = insulin, th = thaumatin) and environment (s = space and g = ground). Table S6: Normalized quality indicators for each dataset; Table S7: Statistics comparing the crystals grown in space and ground conditions; Table S8: Percentage of variance explained by each of the ten dimensions obtained by PCA analysis of the quality indicators; Table T9: Contribution (percent) of each indicator to the five first dimensions.

Author Contributions: J.A.G., F.O., L.A.G.-R., E.M. and J.M.G.-R. designed and set-up the crystallization experiments; J.A.G. and L.A.G.-R. performed the X-ray diffraction experiments and data reduction; F.O. did the statistical analysis of indicators, J.A.G., F.O., A.E.S.v.D., E.M. and J.M.G.-R. wrote the paper. All authors read the manuscript and provided useful comments. All authors have read and agreed to the published version of the manuscript.

Funding: This study was supported by projects ESP2005-23831-E and ESP2007-29071-E (Spanish Ministry of Education and Science) and BIO2016-74875-P (JAG) (MINECO), Spain co-funded by the Fondo Europeo de Desarrollo Regional, FEDER funds, European Union.

Acknowledgments: We are really thankful to Carlos Ruiz (RIP), Carlos A. Nieves and Rafael Estremera from the group of Juan Lopez Garriga, University of Puerto Rico at Mayagüez, for supplying the two hemoglobin proteins and for their assistance during data collection at the ESRF. We are very grateful to the European Synchrotron Radiation Facility for provision of synchrotron radiation facilities and we would like to thank BM16 staff for assistance and support during data collection. We also acknowledged the continuous support of the ESA team, Olivier Minster, Antonio Verga, and Philippe DeGieter (ESA, Noordwijk, NL) and the help of the Russian team at the Integration Hall in Baikonur, Kazakhstan (RKK-Energiya). We would like to thank to Alfonso Garcia-Caballero for revising the manuscript.

Conflicts of Interest: The authors declare no conflicts of interest.

References

1. Scott, T.J.; Vonortas, N.S. Microgravity protein crystallization for drug development: a bold example of public sector entrepreneurship. *J. Tech. Trans.* **2019**, 1–20. [[CrossRef](#)]
2. DeLucas, L.J.; Moore, K.M.; Long, M.M.; Rouleau, R.; Bray, T.; Crysel, W.; Weise, L. Protein crystal growth in space, past and future. *J. Cryst. Growth* **2002**, 237–239, 1646–1650. [[CrossRef](#)]
3. Gonzalez-Ramirez, L.A.; Carrera, J.; Gavira, J.A.; Melero-Garcia, E.; Garcia-Ruiz, J.M. Granada Crystallization Facility-2: A Versatile Platform for Crystallization in Space†. *Cryst. Growth Des.* **2008**, 8, 4324–4329. [[CrossRef](#)]
4. Judge, R.A.; Snell, E.H.; van der Woerd, M.J. Extracting trends from two decades of microgravity macromolecular crystallization history. *Acta Cryst. Sec. D* **2005**, 61, 763–771. [[CrossRef](#)] [[PubMed](#)]
5. Martirosyan, A.; DeLucas, L.J.; Schmidt, C.; Perbandt, M.; McCombs, D.; Cox, M.; Radka, C.; Betzel, C. Effect of macromolecular mass transport in microgravity protein crystallization. *Grav. Space Res.* **2019**, 7, 33–44. [[CrossRef](#)]
6. McPherson, A.; DeLucas, L.J. Microgravity protein crystallization. *npj Microgravity* **2015**, 1. [[CrossRef](#)]
7. Ruyters, G.; Betzel, C. Protein Crystallization in Space: Early Successes and Drawbacks in the German Space Life Sciences Program. *Biotech. Space* **2017**, 11–26. [[CrossRef](#)]
8. Carter, D.C.; Lim, K.; Ho, J.X.; Wright, B.S.; Twigg, P.D.; Miller, T.Y.; Chapman, J.; Keeling, K.; Ruble, J.; Vekilov, P.G.; et al. Lower dimer impurity incorporation may result in higher perfection of HEWL crystals grown in microgravity. *J. Cryst. Growth* **1999**, 196, 623–637. [[CrossRef](#)]
9. Ng, J.D.; Lorber, B.; Giegé, R.; Koszelak, S.; Day, J.; Greenwood, A.; McPherson, A. Comparative Analysis of Thaumatin Crystals Grown on Earth and in Microgravity. *Acta Cryst. Section D Bio. Cryst.* **1997**, 53, 724–733. [[CrossRef](#)]

10. Snell, E.H.; Weisgerber, S.; Helliwell, J.R.; Weckert, E.; Hölzer, K.; Schroer, K. Improvements in lysozyme protein crystal perfection through microgravity growth. *Acta Cryst. Section D Bio. Cryst.* **1995**, *51*, 1099–1102. [[CrossRef](#)]
11. McPherson, A.; Greenwood, A.; Day, J. The effect of microgravity on protein crystal growth. *Adv. Space Res.* **1991**, *11*, 343–356. [[CrossRef](#)]
12. McPherson, A.; Malkin, A.J.; Kuznetsov, Y.G.; Koszelak, S.; Wells, M.; Jenkins, G.; Howard, J.; Lawson, G. The effects of microgravity on protein crystallization: evidence for concentration gradients around growing crystals. *J. Cryst. Growth* **1999**, *196*, 572–586. [[CrossRef](#)]
13. Otálora, F.; Luisa Novella, M.; Rondon, D.; Garca-Ruiz, J.M. Growth of lysozyme crystals under microgravity conditions in the LMS [STS-78] mission. *J. Cryst. Growth* **1999**, *196*, 649–664. [[CrossRef](#)]
14. Thomas, B.R.; Chernov, A.A.; Vekilov, P.G.; Carter, D.C. Distribution coefficients of protein impurities in ferritin and lysozyme crystals Self-purification in microgravity. *J. Cryst. Growth* **2000**, *211*, 149–156. [[CrossRef](#)]
15. Lee, C.P.; Chernov, A.A. Solutal convection around growing protein crystals and diffusional purification in Space. *J. Cryst. Growth* **2002**, *240*, 531–544. [[CrossRef](#)]
16. Snell, E.H.; Judge, R.A.; Crawford, L.; Forsythe, E.L.; Pusey, M.L.; Sportiello, M.; Todd, P.; Bellamy, H.; Lovelace, J.; Cassanto, J.M.; et al. Investigating the Effect of Impurities on Macromolecule Crystal Growth in Microgravity. *Cryst. Growth Des.* **2001**, *1*, 151–158. [[CrossRef](#)]
17. García-Ruiz, J.M.; Otálora, F. Macromolecular Crystals—Growth and Characterization. *Cryst. Growth Fund. Tech.* **2004**, 369–390. [[CrossRef](#)]
18. García-Ruiz, J.M.; Otálora, F.; García-Caballero, A. The role of mass transport in protein crystallization. *Acta Cryst. Sec. F Struc. Bio. Commun.* **2016**, *72*, 96–104. [[CrossRef](#)]
19. Lin, H.; Rosenberger, F.; Alexander, J.I.D.; Nadarajah, A. Convective-diffusive transport in protein crystal growth. *J. Cryst. Growth* **1995**, *151*, 153–162. [[CrossRef](#)]
20. Otálora, F.; García-Ruiz, J.M.; Carotenuto, L.; Castagnolo, D.; Novella, M.L.; Chernov, A.A. Lysozyme crystal growth kinetics in microgravity. *Acta Cryst. Section D Bio. Cryst.* **2002**, *58*, 1681–1689. [[CrossRef](#)]
21. Lorber, B. The crystallization of biological macromolecules under microgravity: a way to more accurate three-dimensional structures? *Biochim. Biophys. Acta [BBA] Proteins Proteomics* **2002**, *1599*, 1–8. [[CrossRef](#)]
22. Vergara, A.; Lorber, B.; Sauter, C.; Giege, R.; Zagari, A. Lessons from crystals grown in the Advanced Protein Crystallisation Facility for conventional crystallisation applied to structural biology. *Biophys Chem* **2005**, *118*, 102–112. [[CrossRef](#)] [[PubMed](#)]
23. Poodt, P.W.G.; Heijna, M.C.R.; Christianen, P.C.M.; van Enkevort, W.J.P.; de Grip, W.J.; Tsukamoto, K.; Maan, J.C.; Vlieg, E. Using Gradient Magnetic Fields to Suppress Convection during Crystal Growth. *Cryst. Growth Des.* **2006**, *6*, 2275–2280. [[CrossRef](#)]
24. Carter, D.C.; Rhodes, P.; McRee, D.E.; Tari, L.W.; Dougan, D.R.; Snell, G.; Abola, E.; Stevens, R.C. Reduction in diffuso-convective disturbances in nanovolume protein crystallization experiments. *J. Appl. Cryst.* **2005**, *38*, 87–90. [[CrossRef](#)]
25. Lavalette, D.; Tétreau, C.; Tourbez, M.; Blouquit, Y. Microscopic Viscosity and Rotational Diffusion of Proteins in a Macromolecular Environment. *Biophys. J.* **1999**, *76*, 2744–2751. [[CrossRef](#)]
26. Ng, J.D.; Gavira, J.A.; García-Ruiz, J.M. Protein crystallization by capillary counterdiffusion for applied crystallographic structure determination. *J. Struc. Bio.* **2003**, *142*, 218–231. [[CrossRef](#)]
27. Otálora, F.; Gavira, J.A.; Ng, J.D.; García-Ruiz, J.M. Counterdiffusion methods applied to protein crystallization. *Progress Biophys. Mol. Bio.* **2009**, *101*, 26–37. [[CrossRef](#)]
28. Poodt, P.W.G.; Heijna, M.C.R.; Schouten, A.; Gros, P.; van Enkevort, W.J.P.; Vlieg, E. Simple Geometry for Diffusion Limited Protein Crystal Growth: Harnessing Gravity to Suppress Convection. *Cryst. Growth Des.* **2009**, *9*, 885–888. [[CrossRef](#)]
29. Ramachandran, N.; Leslie, F.W. Using magnetic fields to control convection during protein crystallization—analysis and validation studies. *J. Cryst. Growth* **2005**, *274*, 297–306. [[CrossRef](#)]
30. Tagami, M.; Hamai, M.; Mogi, I.; Watanabe, K.; Motokawa, M. Solidification of levitating water in a gradient strong magnetic field. *J. Cryst. Growth* **1999**, *203*, 594–598. [[CrossRef](#)]
31. Lorber, B.; Sauter, C.; Theobald-Dietrich, A.; Moreno, A.; Schellenberger, P.; Robert, M.-C.; Capelle, B.; Sanglier, S.; Potier, N.; Giege, R. Crystal growth of proteins, nucleic acids, and viruses in gels. *Prog Biophys Mol Biol* **2009**, *101*, 13–25. [[CrossRef](#)]

32. Moreno, A.; Mendoza, M.E. Crystallization in Gels. In *Handbook of Crystal Growth*, 2nd ed.; Elsevier: Amsterdam, The Netherlands, 2015; pp. 1277–1315.
33. Rizzato, S.; Moret, M.; Merlini, M.; Albinati, A.; Beghi, F. Crystal growth in gelled solution: applications to coordination polymers. *CrystEngComm* **2016**, *18*, 2455–2462. [[CrossRef](#)]
34. Garcia-Ruiz, J.M.; Novella, M.L.; Moreno, R.; Gavira, J.A. Agarose as crystallization media for proteins : I: Transport processes. *J. Cryst. Growth* **2001**, *232*, 165–172. [[CrossRef](#)]
35. Vidal, O.; Robert, M.C.; Boué, F. Gel growth of lysozyme crystals studied by small angle neutron scattering: case of agarose gel, a nucleation promotor. *J. Cryst. Growth* **1998**, *192*, 257–270. [[CrossRef](#)]
36. Chernov, A.A.; Garcia-Ruiz, J.M.; Thomas, B.R. Visualization of the impurity depletion zone surrounding apoferritin crystals growing in gel with holoferritin dimer impurity. *J. Cryst. Growth* **2001**, *232*, 184–187. [[CrossRef](#)]
37. Van Driessche, A.E.S.; Otalora, F.; Gavira, J.A.; Sazaki, G. Is Agarose an Impurity or an Impurity Filter? In Situ Observation of the Joint Gel/Impurity Effect on Protein Crystal Growth Kinetics. *Cryst. Growth Des.* **2008**, *8*, 3623–3629. [[CrossRef](#)]
38. Lorber, B.; Sauter, C.; Ng, J.D.; Zhu, D.W.; Giegé, R.; Vidal, O.; Robert, M.C.; Capelle, B. Characterization of protein and virus crystals by quasi-planar wave X-ray topography: a comparison between crystals grown in solution and in agarose gel. *J. Cryst. Growth* **1999**, *204*, 357–368. [[CrossRef](#)]
39. Garcia-Ruiz, J.M.; Gavira, J.A.; Otálora, F.; Guasch, A.; Coll, M. Reinforced protein crystals. *Mater. Res. Bulletin* **1998**, *33*, 1593–1598. [[CrossRef](#)]
40. Gavira, J.A.; Conejero-Muriel, M.; Delgado-López, J.M. Seeding from silica-reinforced lysozyme crystals for neutron crystallography. *Acta Cryst. Section D Struc. Bio.* **2018**, *D74*, 1200–1207. [[CrossRef](#)]
41. Gavira, J.A.; Garcia-Ruiz, J.M. Agarose as crystallisation media for proteins II: trapping of gel fibres into the crystals. *Acta Cryst. Section D Bio. Cryst.* **2002**, *58*, 1653–1656. [[CrossRef](#)]
42. Gavira, J.A.; Van Driessche, A.E.S.; Garcia-Ruiz, J.-M. Growth of Ultrastable Protein–Silica Composite Crystals. *Cryst. Growth Des.* **2013**, *13*, 2522–2529. [[CrossRef](#)]
43. Dong, J.; Boggon, T.J.; Chayen, N.E.; Raftery, J.; Bi, R.-C.; Helliwell, J.R. Bound-solvent structures for microgravity-, ground control-, gel- and microbatch-grown hen egg-white lysozyme crystals at 1.8 Å resolution. *Acta Cryst. Section D Bio. Cryst.* **1999**, *55*, 745–752. [[CrossRef](#)] [[PubMed](#)]
44. Evrard, C.; Maes, D.; Zegers, I.; Declercq, J.-P.; Vanhee, C.; Martial, J.; Wyns, L.; Weerd, C.V.D. TIM Crystals Grown by Capillary Counterdiffusion: Statistical Evidence of Quality Improvement in Microgravity. *Cryst. Growth Des.* **2007**, *7*, 2161–2166. [[CrossRef](#)]
45. Miller, T.Y.; He, X.-m.; Carter, D.C. A comparison between protein crystals grown with vapor diffusion methods in microgravity and protein crystals using a gel liquid-liquid diffusion ground-based method. *J. Cryst. Growth* **1992**, *122*, 306–309. [[CrossRef](#)]
46. Kundrot, C.E.; Judge, R.A.; Pusey, M.L.; Snell, E.H. Microgravity and Macromolecular Crystallography. *Cryst. Growth Des.* **2001**, *1*, 87–99. [[CrossRef](#)]
47. Snell, E.H.; Helliwell, J.R. Macromolecular crystallization in microgravity. *Rep. Prog. Phys* **2005**, *68*, 799–853. [[CrossRef](#)]
48. Otwinowski, Z.; Minor, W. Processing of X-ray diffraction data collected in oscillation mode. *Methods Enzymol.* **1997**, *276*, 307–326.
49. Carotenuto, L.; Cartwright, J.H.E.; Castagnolo, D.; García Ruiz, J.M.; Otálora, F. Theory and simulation of buoyancy-driven convection around growing protein crystals in microgravity. *Micrograv. Sci. Tech.* **2002**, *13*, 14–21. [[CrossRef](#)]
50. Caylor, C.L.; Dobrianov, I.; Lemay, S.G.; Kimmer, C.; Kriminski, S.; Finkelstein, K.D.; Zipfel, W.; Webb, W.W.; Thomas, B.R.; Chernov, A.A.; et al. Macromolecular impurities and disorder in protein crystals. *Proteins: Struc. Funct. Gene.* **1999**, *36*, 270–281. [[CrossRef](#)]
51. Yoshizaki, I.; Sato, T.; Igarashi, N.; Natsuisaka, M.; Tanaka, N.; Komatsu, H.; Yoda, S. Systematic analysis of supersaturation and lysozyme crystal quality. *Acta Cryst. Sec. D Bio. Cryst.* **2001**, *57*, 1621–1629. [[CrossRef](#)]
52. Jones, L.V. *The Collected Works of John W. Tukey: Philosophy and Principles of Data Analysis 1965-1986*; Taylor & Francis: London, UK, 1987.
53. Maes, D.; Evrard, C.; Gavira, J.A.; Sleutel, M.; Van De Weerd, C.; Otalora, F.; Garcia-Ruiz, J.M.; Nicolis, G.; Martial, J.; Decanniere, K. Toward a definition of x-ray crystal quality. *Cryst. Growth Des.* **2008**, *8*, 4284–4290. [[CrossRef](#)]

54. Mardia, K.V.; Kent, J.T.; Bibby, J.M. *Multivariate Analysis*; Academic Press: London, UK, 1979.
55. Venables, W.N.; Ripley, D.R. *Modern Applied Statistics with S*; Springer-Verlag: New York, NY, USA, 2002.



© 2020 by the authors. Licensee MDPI, Basel, Switzerland. This article is an open access article distributed under the terms and conditions of the Creative Commons Attribution (CC BY) license (<http://creativecommons.org/licenses/by/4.0/>).